Structural basis for the regulatory role of the PPxY motifs in the thioredoxin-interacting protein TXNIP[§]

Yanli Liu[a, b#], Johnathan Lau[b#], Weiguo Li[b, c], Wolfram Tempel[b], Li Li[b], Aiping Dong[b], Ashrut Narula[b], Su Qin[b, d*] and Jinrong Min[a, b, e*]

[a] Hubei Key Laboratory of Genetic Regulation and Integrative Biology, College of Life Science, Central China Normal University, Wuhan 430079, PR China.
[b] Structural Genomics Consortium, University of Toronto, 101 College Street, Toronto, Ontario M5G 1L7, Canada.
[c] Key Laboratory of Pestcide & Chemical Biology, College of Chemistry, Central China Normal University, Wuhan 430079, PR China.
[d] Materials Characterization and Preparation Center and Life Science Research Center, South University of Science and Technology of China, Shenzhen 518055, China.
[e] Department of Physiology, University of Toronto, Toronto, Ontario M5S 1A8, Canada

[§]Running title: Structural basis for the regulatory roles of PPxY motifs in TXNIP

[#] These authors contributed equally to the work.
***** To whom correspondence should be addressed. Tel: 416-9463868 Fax: 416-9460880 Email: jr.min@utoronto.ca
Correspondence may also be addressed to Su Qin. Tel: 416-9299353 Fax: 416-9460880 Email: qinsu08@gmail.com

ABSTRACT

Thioredoxin interacting protein (TXNIP) negatively regulates the antioxidative activity of thioredoxin, and participates in pleiotropic cellular processes. Its deregulation is linked to various human diseases including diabetes, acute myeloid leukemia and cardiovascular diseases. The E3 ubiquitin ligase Itch polyubiquitinates TXNIP to promote its degradation via the ubiquitin proteasome pathway, and this Itch-mediated poly-ubiquitination of TXNIP is dependent on the interaction of the four WW domains of Itch with the two PPxY motifs of TXNIP. However, the molecular mechanism of this interaction of TXNIP with Itch remains elusive. In this study, we found that each of the four WW domains of Itch exhibited different binding affinities to TXNIP, while multivalent engagement between the four WW domains of Itch and the two PPxY motifs of TXNIP resulted in their strong binding avidity. Our structural analyses demonstrated that the third and fourth WW domains of Itch were able to recognize both PPxY motifs of TXNIP simultaneously, supporting a multivalent binding mode between Itch and TXNIP. Interestingly, phosphorylation status on the tyrosine residue of the PPxY motifs of TXNIP serves as a molecular switch in its choice of binding partners and thereby downstream biological signaling outcomes. Phosphorylation of this tyrosine residue of TXNIP diminished the binding capability of PPxY motifs of TXNIP to Itch, whereas this phosphorylation is a prerequisite to the binding activity of TXNIP to SH2 domain containing protein SHP2 and their roles in stabilizing the phosphorylation and activation of CSK.

Summary statement

Itch[1] directly binds to and negatively regulates TXNIP. Structural studies revealed the regulatory role of the PPxY motifs in TXNIP: TNXIP binds to Itch through multivalent interactions, while phosphorylation of TNXIP switched its binding to SH2 protein SHP2.

Key words: TXNIP, PPxY motifs, Itch, SHP2, phosphotyrosine

INTRODUCTION

Thioredoxin-interacting protein (TXNIP) together with α-arrestin domain-containing proteins 1-5 (ARRDC1-5) constitute the α-arrestin family. A shared characteristic feature of ARRDC2, 3, 4 and TXNIP is that they all possess two highly conserved C-terminal PPxY motifs (Figure 1A) [1-3]. TXNIP is initially recognized as an important modulator of the redox system [2]. In the cytoplasm, TXNIP inhibits the endogenous antioxidative function of thioredoxin-1, allowing oxidative stress to accumulate in the cell [4, 5]. In the mitochondria, TXNIP binds to thioredoxin-2, and promotes phosphorylation and activation of Apoptosis Signal-Regulating Kinase 1 (ASK1), leading to cytochrome C release from the mitochondria and eventual apoptosis [6]. TXNIP also plays a critical role in glucose and lipid metabolism and is an important tumor-suppressor in various cancers [5, 7-10]. Consistent with its critical roles in diverse cellular processes, TXNIP is tightly regulated at multiple levels [3, 11]. Intracellular stability of TXNIP is controlled via the ubiquitin-proteasome pathway [12]. The E3 ubiquitin protein ligase Itchy homolog (Itch) negatively regulates TXNIP, as Itch over-expression increases rates of polyubiquitination and proteasomal degradation of TXNIP. Correspondingly, intracellular TXNIP levels increase when Itch is knocked down [12]. Therefore, Itch-mediated degradation of TXNIP serves as an important means to modulate TXNIP protein levels, and thus fine-tunes the activity of TXNIP in oxidative stress, metabolism, and apoptosis [13]. Given its involvement in multiple important signaling pathways, dysregulation of TXNIP has been linked to several human diseases, including cardiovascular diseases [14] and cancers especially acute myeloid leukemia [15].

Itch belongs to the Nedd4-like family of E3 ubiquitin ligases, which all share three conserved regions: a Ca^{2+}/ lipid-binding (C2) domain in the N-terminus, 2-4 WW domains in the middle and a HECT-type catalytic ligase domain in the C-terminus (Figure 1A) [16]. The C2 domain targets membranes and membrane proteins [17], the HECT domain accepts ubiquitin from E2 ubiquitin-conjugating enzymes [18], and the WW domains determine substrate selectivity through specific interactions with amino acid sequence motifs in target proteins [19]. The WW domain is a ubiquitous structural and functional unit found in a large number of otherwise unrelated proteins [20]. The WW domains present in E3 ligases typically belong to group I, which is defined by the ability to target ligands containing a PPxY motif, which in turn is critical for Itch-TXNIP interactions [19, 21]. The four WW domains of Itch bind to the two PPxY motifs of TXNIP. These structural domains and motifs do not contribute equally to the interaction and the subsequent Itch-mediated degradation of TXNIP [12]. Details of the molecular mechanism remain unclear. The tyrosine residue of the PPxY motif may undergo phosphorylation, an important posttranslational modification for regulating cellular signaling pathways [22]. This tyrosine phosphorylation mark can be read by a large number of protein domains, such as the SH2 and BRCT domains [23], but how it can modulate the interaction and function of TXNIP has not been reported yet. A recent study showed that TXNIP's PPTY motif binds to SH2 domains of Src homology phosphatase-2 (SHP2), which prevents the dephosphorylation and deactivation of CSK, while mutation from PPTY to PPTA disrupts this interaction [24]. However, whether this interaction depends on tyrosine phosphorylation is not clear.

Here we show that although all four WW domains of Itch displayed binding activities to both PPxY motifs of TXNIP, their respective binding affinities varied

drastically, from the micromolar to millimolar range. The simultaneous engagement of multiple domains significantly enhanced the binding between Itch and TXNIP, suggesting multivalent binding as a mechanism governing selectivity and affinity. We also solved the high-resolution crystal structure of the complex formed by the Itch WW3-WW4 tandem domains and the PPCY motif of TXNIP. Moreover, we found that tyrosine phosphorylation of PPxY motifs in TXNIP abolished its binding activity to Itch, but promoted its interaction with SHP2, demonstrating that tyrosine phosphorylation of PPxY motifs of TXNIP plays a key role in dictating the choices of binding partners of TXNIP and thereby the downstream biological signaling outcomes.

EXPERIMENTAL PROCEDURES

Protein expression and purification

The DNA fragments corresponding to four WW domains (WW1, residues 324-362; WW2, residues 356-394; WW3, residues 436-474; WW4, residues 475-514) of Itch and tandem WW1-WW2 domains (residues 324-394), tandem WW3-WW4 domains (residues 433-521), tandem WW1-WW4 domains (residues 324-521) were subcloned into a modified pET28-GST vector to generate N-terminal GST, His-tagged fusion protein. The DNA fragment corresponding to native TXNIP peptide with two PPxY motifs (residues 327-382) was subcloned into a modified pET28-MHL vectors to generate N-terminal His-tagged fusion proteins. The plasmids of N terminal (residues 1-104), C terminal (residues 101-222) and tandem (residues 1-222) SH2 domains of SHP2 were generously provided by Dr. Karen Colwill (Lunenfeld-Tanenbaum Research Institute, Mount Sinai Hospital). Recombinant proteins were overexpressed in *Escherichia coli* BL21 (DE3) Codon plus RIL (Stratagene) at 15 °C and purified by affinity chromatography on Ni-nitrilotriacetate resin (Qiagen) followed by thrombin or TEV protease treatment to remove the tag. The protein was further purified on a Superdex75 gel-filtration column (GE Healthcare, Piscataway, NJ). For crystallization experiments, purified protein was concentrated to 10 mg/mL in a buffer containing 20 mM Tris, pH 7.5, 150 mM NaCl and 1 mM DTT.

Isothermal Titration Calorimetry (ITC)

All TXNIP peptides, except native TXNIP peptide with two PPxY motifs, were synthesized by Peptide 2.0 Inc. For ITC measurements, the concentrated proteins were diluted in 20 mM Tris, pH 7.5, and 150 mM NaCl. Likewise, the lyophilized peptides were dissolved in the same buffer and pH was adjusted by adding NaOH. Tyrosine-containing peptide concentrations were estimated with absorbance spectroscopy using the extinction coefficient, $\varepsilon 280 = 1280 M^{-1}\ cm^{-1}$. All measurements except those of binding between tandem WW1-WW2 and 2_PPxY_short peptide were performed at 25 ºC, using a VP-ITC microcalorimeter. Protein with a concentration of 50-100 μM was placed in the cell chamber, and the peptides with a concentration of 1-3 mM in syringe were injected in 25 successive injections with a spacing of 180 s and a reference power of 13 mcal/s. Control experiments were performed under identical conditions to determine the heat signals that arise from injection of the peptides into the buffer. Data were fitted using the single-site binding model within the Origin software package (MicroCal, Inc.).

Due to limited protein yield, the WW1-WW2 ITC was performed using a Nano-ITC microcalorimeter (TA, Inc). The binding data should be consistent with those from the

regular ITC instrument, confirmed by ITC results of WW3-WW4 using both regular and Nano-ITC instruments. GST, His-tagged fusion protein with a concentration of 50 μM was placed in the cell chamber, and 2_PPxY_short peptide (lacking the linker sequence between the two PPxY motifs) with a concentration of 0.5 mM was injected in 25 successive injections with a spacing of 120 s at 25 ºC. Control experiments were performed under identical conditions to determine the heat signals that arise from injections of the peptide into the buffer or into the GST, His-tag only protein. Data were fitted using the independent model within the NanoAnalyze software package (TA, Inc.).

NMR sample preparation and NMR spectroscopy

Uniformly ^{15}N-labeled proteins were prepared by growing bacteria in M9 media using $^{15}NH_4Cl$ (0.5 g/liter) as stable isotope source. The purified ^{15}N-labeled tandem WW3-WW4 domains proteins were dissolved to a final concentration of 0.25 mM in a buffer containing 20 mM Tris, pH 7.5, 150 mM NaCl and 10% D_2O. All NMR experiments were performed at 298 K on a Bruker DMX500 spectrometer. ^{1}H-^{15}N HSQC spectra of Itch protein in the free state or in the presence of TXNIP peptides were recorded. The assignment of Q465 was extracted from a previous study [25].

Protein crystallization

Purified protein was mixed with TXNIP peptides at a 1:3 molar ratio and crystallized using the sitting drop vapor diffusion method at 20 ºC after mixing 0.5 μL of the protein solution with 0.5 μL of the reservoir solution. Crystals were obtained with a reservoir solution containing 30% PEG 4000, 0.2 M magnesium chloride, 0.1 M Tris HCI, pH 8.5 for tandem (WW3-WW4)-PPCY; 20% PEG-3350, 0.2 M ammonium formate for SHP2-SH2 with PPTpY peptide. Before flash-freezing crystals in liquid nitrogen, crystals were soaked in a cryoprotectant consisting of 85% reservoir solution and 15% glycerol.

Data collection and structure determination

Diffraction data were collected at the Advanced Photon Source beam line 19ID. Intensities of symmetry-related reflections were merged with AIMLESS [26]. PHASER [27] was used for molecular replacement. ARP/WARP [28] was used for automated model building. COOT [29], JLIGAND [30], REFMAC [31], PHENIX/MOLPROBITY [32, 33] were used for molecular model building, restraint preparation, restrained model refinement and geometry validation, respectively. Information pertaining to individual crystal structures is summarized in footnote 2.

PDB_EXTRACT [34] was used to prepare the models for PDB deposition. The IOTBX library [35], PHENIX and CCP4 [36] programs were used to summarize information for Table 1. Figures of molecular models were generated with PyMOL (Schrödinger, LLC). Potential surfaces were calculated using PyMOL's built-in vacuum electrostatics function.

RESULTS AND DISCUSSION

WW domains of Itch bind to PPxY motifs of TXNIP with varying affinities

Previous studies have shown that the WW domains of Itch interact with the PPxY motifs in the C-terminus of TXNIP [12]. To elucidate specific determinants of this interaction, we performed isothermal titration calorimetry (ITC) assays using synthetic peptides and

recombinant proteins of WW domains (Figure 1). Therein, all four WW domains of Itch bound to both PPxY motifs of TXNIP. However, their binding affinities varied, depending on both the WW domains and PPxY motifs (Figure 1B and Supplementary Figure S1A and S1B). The first two WW domains (WW1 and WW2) bound to either PPxY motif of TXNIP more strongly than the last two WW domains (WW3 and WW4) (Figure 1B and Supplementary Figure S1A and S1B).

Multivalent engagement of different WW domains and PPxY motifs produce a strong binding avidity

Many proteins contain multiple WW domains that may increase selectivity and affinity for ligands or enhance the proteins' functional diversity by their ability to bind peptide sequences from different proteins. To study the effects of multivalent interactions of the tandem WW domains of Itch on the binding affinity, we performed a series of ITC assays (Figure 1B and Supplementary Figure S1C). We were able to express stable proteins for both WW1-WW2 and WW3-WW4 constructs, but for the WW1-WW2 construct, we were unable to remove the GST tag and the protein yield was low. Nevertheless, the GST tag should not affect the WW binding ability because in control experiments, the GST tag did not bind to any peptides used in the study (data not shown). Due to the limitations of our WW1-WW2 protein preparation, we resorted to use tandem WW3-WW4 protein for most of our assays. A TXNIP peptide containing both PPCY and PPTY motifs (2_PPxY_short, tandem PPxY peptide that lacks the linker sequence between these 2 PPxY motifs) bound to the tandem WW1-WW2 or WW3-WW4 domains significantly more tightly than any single PPxY peptide bound to either individual Itch WW domain (Figure 1B and Supplementary Figure S1C). Although single WW1 and WW2 showed higher binding affinities than single WW3 and WW4, tandem WW domains (WW1-WW2 or WW3-WW4) bound to peptides containing 2 PPxY motifs with similar affinities, suggesting that either tandem may play a role in the interaction between Itch and TXNIP. As a control, we measured the binding affinity of the recombinant TXNIP fragment containing both PPCY and PPTY motifs with the linker sequence (2_PPxY_long) and performed ITC against the tandem WW3-WW4 domains (Figure 1B and Supplementary Figure S1C). The observed affinity was comparable to that of the short TXNIP peptide, suggesting that the linker sequence between the motifs was not crucial for multivalent interactions, similar to a previous report on FBP21 protein [37]. Taken together, these results suggest that multivalent engagement of WW domains and PPxY motifs generates a strong binding avidity between TXNIP and Itch.

This multivalent binding mode is consistent with previous findings that binding of full length ARRDC3 (a homolog of TXNIP) and Nedd4 (another member of E3 ubiquitin ligases) is mediated by interactions between both of ARRDC3's PPxY motifs and Nedd4's WW2-WW3 or WW3-WW4 tandem WW domains [38]. Accordingly, although single mutant in WW3 weakens the interaction, double or triple mutants in tandem WW2-WW3, WW3-WW4 or WW2-WW3-WW4 almost abrogates the interaction, what is also confirmed by co-immunoprecipitation assay in HEK293 cells [38], underlining the importance of multivalent interactions between TXNIP and Itch. The strength of the interaction is also similar to Nedd4's, which showed sub-micromolar binding affinities to ENaC or ARRDC3 as well [38, 39]. The presence of multiple binding sites in these proteins balances between the requirements of dynamic regulation and stabilization of a

specific interaction at a locus after initial recruitment. In conclusion, combinations of multiple interacting domains can greatly increase substrate selectivity, binding strength and adaptability of the interaction. Importantly, the multivalent engagement may explain why both PPxY motifs are required for Itch to polyubiquitinate TXNIP, as deletion of either motif abrogates TXNIP proteasomal degradation due to decreased selectivity and affinity [12].

It is still not clear how the four WW domains of Itch interact with two PPxY motifs of TXNIP, since we could not generate protein containing all four WW domains of Itch, preventing us from performing corresponding binding and structural studies. Considering that tandem WW domains WW1-WW2 and WW3-WW4 exhibited similar binding affinities to peptides containing both PPxY motifs, it is conceivable that the full length Itch protein should have comparable binding ability to TXNIP as the tandem WW domains do, and any two WW domains from the four WW domains might recognize the two PPxY motifs simultaneously, although we favor a model in which four WW domains formed two functional units, such as WW1-WW2 and WW3-WW4, and each of them could recognize both PPxY motifs *in vivo*, which would double the possibility of the initial recruitment of TXNIP by Itch. We observed a similar phenomenon for the methyl-arginine Tudor binding protein SND1, in which multiple methyl-arginine sites do not significantly enhance its binding to SND1, but would increase the possibility of initial recruitment of the Tudor protein SND1 [40].

The presence of two binding sites between the tandem WW domains and the bivalent PPxY peptide raised the question as to which relative orientation between the bivalent TXNIP peptide and the bivalent Itch WW domains was preferred. To address this question, we performed NMR chemical shift perturbation experiments with tandem WW3-WW4, which we could isotopically label for NMR study. The NMR titration revealed that a peak corresponding to the WW3 residue Q465, a residue in the XP groove (see below), moved in different directions upon addition of PPCY or PPTY peptides (Supplementary Figure S2A). One possible interpretation is that WW3 domain of Itch bound to the PPCY motif and the WW4 domain bound to the PPTY motif in the context of these tandem WW domains (Supplementary Figure S2B).

Structural basis for the PPxY motif recognition by Itch WW domains

To uncover the molecular basis of the interaction between the Itch WW domains and the TXNIP PPxY motifs at atomic resolution, we determined the crystal structure of tandem WW3-WW4 domains (residues 433-521) in complex with the TXNIP PPCY peptide at 1.40 Å resolution (Table 1). The WW domains adopted the canonical conformation of a twisted triple-stranded anti-parallel β-sheet, with the PPCY peptide packing against the concave side of the β-sheet and aligning approximately in parallel with the middle β-strand of the WW domain, similar to observations in other WW-PPxY complex structures [38, 41] (Figures 2). Since the single WW domains show strong sequence similarity (Figure 2A) and both tandem WW domains (WW1-WW2 and WW3-WW4) showed similar binding affinities to TXNIP (Figure 1B), the structure should be representative for the interaction between Itch and TXNIP.

The PPCY peptide has the sequence *N*-TPEAPPCYMDVI-*C*, corresponding to residues 327′-338′ of TXNIP (hereafter, TXNIP residue numbers are marked with a prime (′) to distinguish them from the Itch residue numbers) (Figure 1A). In the (WW3-

WW4)-PPCY complex, the substructures of WW3-PPCY and WW4-PPCY are similar; we shall refer to the WW3-PPCY component of (WW3-WW4)-PPCY complex in the following discussion. The residues P331' and P332' of the PPCY peptide form a polyproline type II helix [42], whereas residues 334′-337′ adopt a helical fold (Figure 2B). The binding site of the peptide is located on one face of the WW sheet and consists of two canonical grooves, namely the XP groove and tyrosine-binding groove (Tyr groove) (Figure 2). P331′ and P332′ insert into the XP groove by stacking against the conserved W466 and Y455 residues of WW3, respectively (Figures 2A and 2B). The side chain of Y334′ is accommodated in the Tyr groove formed by the conserved residues V457, H459 and R462 of WW3 (Figure 2B). In addition to the hydrophobic packing, some hydrogen bonds between the peptide and WW domains contribute to the stabilization of the complex, for example between the carbonyl of P332′ and the hydroxyl of T464, along with the phenolic hydroxyl of Y334′ and Nπ of H459 (Figure 2B). The interaction between P332′ and T464 is indispensable, since phosphorylation of T664 destroys the binding between Itch WW3 domain and LMP2A PPxY peptide [25].

Phosphorylation inhibits the binding of TXNIP to Itch but enables recruitment of SH2 domain containing proteins

The PPxY motif is often subject to phenol phosphorylation, a ubiquitous mechanism that regulates activity and function of proteins. Indeed, Y378′ of the TXNIP PPTY motif can be phosphorylated *in vivo* [43, 44]. How would phosphorylation affect TXNIP binding to WW domains? In our ITC assays, no binding was observed between the phosphorylated PPCY (PPCpY) peptide and tandem WW3-WW4 domains (Figure 3A and Supplementary Figure S3), indicating that phosphorylation of the PPxY motif would abolish the interaction between TXNIP and Itch. On the basis of the crystal structure of the WW domains and PPCY peptide complex, phosphorylation would disrupt the hydrogen bond between residue Y334′ and H459/H499 and cause steric hindrance.

Does phosphorylation of the PPxY motif enable recognition by other proteins? There are a number of phosphorylation readers, including the SH2 domain, BRCT domain and 14-3-3 proteins. The SH2 domain is a sequence-specific phosphotyrosine-binding module present in many signaling molecules. Significantly, the TXNIP's PPTY motif binds to SH2 domains of SHP2 (Src homology phosphatase-2), which prevents the dephosphorylation and deactivation of CSK [24]. According to the PhosphositePlus server, PPTY's tryrosine may be subject to phosphorylation [43, 44], but whether this interaction between SHP2 and TXNIP requires tyrosine phosphorylation is not clear. Tyrosine phosphorylation within the PPxY motifs of β-dystroglycan has been shown to block interaction with the WW domains of dystrophin and utrophin, while promoting the recruitment of SH2 domain-containing proteins [22]. Thus, we performed ITC assays for the N-terminal, C-terminal, and tandem SH2 domains of SHP2 to different tyrosine-phosphorylated or non-phosphorylated PPxY peptides. All these SH2 domains of SHP2 showed moderate binding to the tyrosine-phosphorylated TXNIP peptides, and the binding depended on the phosphorylation mark (Figure 3A). It remains unclear whether the observed binding between tandem SH2 domains and tandem PPx(pY) motifs represents a multivalent interaction and whether a putative multivalent interaction would be physiologically relevant.

We crystallized the tandem SH2 domains of SHP2 (residues 1-222) in complex with

the PPTpY peptide (Figures 3B) and determined the crystal structure. In the crystallographic model, each SH2 domain binds one PPTpY peptide using similar binding modes (Supplementary Figure S3A); thus the C-terminal SH2-PPTpY complex will be used in the following discussion. The SH2 domain of SHP2 adopts the characteristic SH2 fold, which consists of a core anti-parallel β-sheet (βB-βD), two α-helices (αA and αB), which pack on opposite faces of the sheet, respectively, and a cap element formed by another small anti-parallel β-sheet (C terminal βD and βE, and a loop instead of βE in our SHP2 model). To facilitate the comparison, we used the secondary structure notation introduced previously for Src and Lck [45, 46]. We did not observe the N-terminal βA, βE, βF, and C-terminal βG strands seen in other SH2 domains [45, 46]. The peptide is bound in an extended conformation roughly perpendicular to the central β-strands of the SH2 domain (Figure 3B and Supplementary Figure S4B). This binding mode is highly conserved in other SH2 domains [45-50].

According to our complex structure and ITC results, the phosphorylation of the tyrosine residue in the PPxY motif appears indispensable for complex formation as the unmodified PPxY peptide showed no detectable binding to the SH2 domain of SHP2 (Figure 3A). Taken together, our study suggests a novel regulatory role for the PPxY motifs of TXNIP: the phosphorylation mark on the tyrosine not only turns off the signal for Itch-mediated degradation, but also turns on a signal to recruit SH2 domain containing proteins (Figures 3A and 3C). Phosphorylated PPxY motifs of TXNIP bind to SH2 domains of SHP2, which prevents the dephosphorylation and deactivation of CSK [24], although it remains to be investigated if any other SH2-domain containing proteins in addition to SHP2 are physiological targets of TXNIP.

These new data on the function of PPxY motifs have implications for the regulation of cell signaling pathways in which TXNIP participates. For the interaction between Itch and TXNIP, which regulates the degradation of TXNIP, we propose a multivalent binding model. The model requires further refinement and validation, including the identification of specific pairs of WW domains and PPxY motifs that interact *in vivo*. Phosphorylation of tyrosine in PPxY motifs of TXNIP would block TXNIP's interaction with Itch, but promote recruitment SH2 containing proteins such as SHP2. This phosphorylation-dependent switch is reminiscent of our previous report, in which phosphorylation of serine 350 of the PxLPxl/L motif of HDAC4 reduced the binding of ANKRA2 but recruited 14-3-3 proteins for binding with a strong affinity [51]. Furthermore, this phosphorylation-status dependent recognition of PPxY motifs of TXNIP by the WW domains of Itch probably plays important functional roles in cellular signaling pathways *in vivo*, similar to the importance of phosphorylation of Smad that modulates its binding affinities to the WW domains of transcriptional partners such as YAP and Pin1, consequently impacting on the BMP and TGF-β signaling pathways [52]. If one considers TXNIP as a node in the regulatory network of interacting proteins, interaction with SH2 domains should define a significant portion TXNIP's connectivity within that network. Whereas the number of potential direct or indirect effects on cellular processes is vast, TXNIP's SH2-containing "neighbors" in the network context have yet to be exhaustively identified and characterized, and the associated WW-SH2 affinity switch's function clarified in the contexts of cellular homeostasis and pathogenesis.

ACCESSION NUMBERS

Coordinates and structure factors of Itch WW3-WW4-PPCY and SHP2 SH2-PPTpY were deposited under PDB IDs: 5CQ2 and 5DF6, respectively.

ACKNOWLEDGMENTS

We are grateful to Dr. Sachdev Sidhu and Dr. Karen Colwill for the generous gift of constructs of single WW domains of Itch and SH2 domains of SHP2. We thank Dr. Scott Houliston for performing the NMR experiment and Dr. John Walker for suggestions on crystallographic model refinement. Some results shown in this report are derived from work performed at Argonne National Laboratory, Structural Biology Center at the Advanced Photon Source. Argonne is operated by UChicago Argonne, LLC, for the U.S. Department of Energy, Office of Biological and Environmental Research under contract DE-AC02-06CH11357.

CONFLICTS OF INTEREST

The authors declare no conflict of interest.

FUNDING

The SGC is a registered charity (No. 1097737) that receives funds from AbbVie, Boehringer Ingelheim, the Canadian Institutes of Health Research (CIHR), Genome Canada, Ontario Genomics Institute Grant OGI-055, GlaxoSmithKline, Janssen, Lilly Canada, the Novartis Research Foundation, the Ontario Ministry of Economic Development and Innovation, Pfizer, Takeda, and Wellcome Trust Grant 092809/Z/10/Z. This study was also supported by the project of Hubei Key Laboratory of Genetic Regulation and Integrative Biology (GRIB201403), research funds of CCNU from the college's basic research and operation of MOE (No. CCNU15A05036) and National Natural Science Foundation of China (31500613 and 21272090).

AUTHOR CONTRIBUTIONS

Yanli Liu, Johnathan Lau and Weiguo Li purified, crystallized the protein; Yanli Liu, Weiguo Li and Ashrut Narula conducted the ITC assays; Wolfram Tempel collected diffraction data and determined the Itch crystal structure; Aiping Dong determined the SHP2 crystal structure; Jinrong Min conceived and designed the study; Yanli Liu, Johnathan Lau, Li Li, Su Qin and Jinrong Min wrote the paper. All authors approved the final version of the manuscript.

FOOTNOTES

[1] The abbreviations used are: TXNIP, thioredoxin interacting protein; Itch, E3 ubiquitin protein ligase Itchy homolog; SHP2, Src homology phosphatase-2; PPTpY, PPTY phosphorylated on tyrosine.

[2] *Itch-WW3-WW4:* Initially, diffraction intensities were measured on a rotating copper anode and integrated and scaled with DENZO and SCALEPACK [53], respectively. The structure was solved by molecular replacement using preliminary coordinates of the WW3 crystal structure from this laboratory (PDB code 5DWS). ARP/WARP was used for map improvement [54] and automated model building. Synchrotron diffraction data of an isomorphous crystal were reduced with XDS [55] and used for further refinement of

the crystallographic model. *SHP2-SH2:* Synchrotron diffraction data were reduced with DENZO and SCALEPACK. Models for molecular replacement based on PDB entries 3TKZ [48] and 4XZ0 [56] were prepared using the FFAS03 server [57] and SCWRL [58]. ARP/wARP was used for phase improvement and automated model building. JLIGAND [30], the GRADE server (http://grade.globalphasing.org) and MOGUL [59] were used for restraint preparation.

REFERENCES

1 Patwari, P., Higgins, L. J., Chutkow, W. A., Yoshioka, J. and Lee, R. T. (2006) The interaction of thioredoxin with Txnip. Evidence for formation of a mixed disulfide by disulfide exchange. J. Biol. Chem. **281**, 21884-21891

2 Patwari, P., Chutkow, W. A., Cummings, K., Verstraeten, V. L., Lammerding, J., Schreiter, E. R. and Lee, R. T. (2009) Thioredoxin-independent regulation of metabolism by the alpha-arrestin proteins. J. Biol. Chem. **284**, 24996-25003

3 Shalev, A. (2014) Minireview: Thioredoxin-interacting protein: regulation and function in the pancreatic beta-cell. Mol. Endocrinol. **28**, 1211-1220

4 Schulze, P. C., Yoshioka, J., Takahashi, T., He, Z., King, G. L. and Lee, R. T. (2004) Hyperglycemia promotes oxidative stress through inhibition of thioredoxin function by thioredoxin-interacting protein. J. Biol. Chem. **279**, 30369-30374

5 Chen, J., Saxena, G., Mungrue, I. N., Lusis, A. J. and Shalev, A. (2008) Thioredoxin-interacting protein: a critical link between glucose toxicity and beta-cell apoptosis. Diabetes. **57**, 938-944

6 Saxena, G., Chen, J. and Shalev, A. (2010) Intracellular shuttling and mitochondrial function of thioredoxin-interacting protein. J. Biol. Chem. **285**, 3997-4005

7 Goldberg, S. F., Miele, M. E., Hatta, N., Takata, M., Paquette-Straub, C., Freedman, L. P. and Welch, D. R. (2003) Melanoma Metastasis Suppression by Chromosome 6 Evidence for a Pathway Regulated by CRSP3 and TXNIP. Cancer Res. **63**, 432-440

8 Oka, S., Liu, W. R., Masutani, H., Hirata, H., Shinkai, Y., Yamada, S., and Yoshida, T., Nakamura, H., and Yodoi, J. . (2006) Impaired fatty acid utilization in thioredoxin binding protein-2 (TBP-2)-deficient mice: a unique animal model of Reye syndrome. FASEB J. **20**, 121–123

9 Sheth, S., Bodnar, J., Ghazalpour, A., Thipphavong, C., Tsutsumi, S., Tward, A., Demant, P., Kodama, T., Aburatani, H. and Lusis, A. (2006) Hepatocellular carcinoma in Txnip-deficient mice. Oncogene. **25**, 3528-3536

10 Hui, S. T., Andres, A. M., Miller, A. K., Spann, N. J., Potter, D. W., Post, N. M., Chen, A. Z., Sachithanantham, S., Jung, D. Y. and Kim, J. K. (2008) Txnip balances metabolic and growth signaling via PTEN disulfide reduction. Proc. Natl. Acad. Sci. U.S.A. **105**, 3921-3926

11 Chong, C. R., Chan, W. P., Nguyen, T. H., Liu, S., Procter, N. E., Ngo, D. T., Sverdlov, A. L., Chirkov, Y. Y. and Horowitz, J. D. (2014) Thioredoxin-interacting protein: pathophysiology and emerging pharmacotherapeutics in cardiovascular disease and diabetes. Cardiovasc. Drugs Ther. **28**, 347-360

12 Zhang, P., Wang, C., Gao, K., Wang, D., Mao, J., An, J., Xu, C., Wu, D., Yu, H., Liu, J. O. and Yu, L. (2010) The ubiquitin ligase itch regulates apoptosis by targeting thioredoxin-interacting protein for ubiquitin-dependent degradation. J. Biol. Chem. **285**, 8869-8879

13 Xiao, N., Eto, D., Elly, C., Peng, G., Crotty, S. and Liu, Y. C. (2014) The E3 ubiquitin ligase Itch is required for the differentiation of follicular helper T cells. Nat. Immunol. **15**, 657-666

14 Yoshioka, J., Chutkow, W. A., Lee, S., Kim, J. B., Yan, J., Tian, R., Lindsey, M. L., Feener, E. P., Seidman, C. E., Seidman, J. G. and Lee, R. T. (2012) Deletion of thioredoxin-interacting protein in mice impairs mitochondrial function but protects the myocardium from ischemia-reperfusion injury. J. Clin. Invest. **122**, 267-279

15 Zhou, J., Bi, C., Cheong, L. L., Mahara, S., Liu, S. C., Tay, K. G., Koh, T. L., Yu, Q. and Chng, W. J. (2011) The histone methyltransferase inhibitor, DZNep, up-regulates TXNIP, increases ROS production, and targets leukemia cells in AML. Blood. **118**, 2830-2839
16 Bernassola, F., Karin, M., Ciechanover, A. and Melino, G. (2008) The HECT family of E3 ubiquitin ligases: multiple players in cancer development. Cancer Cell. **14**, 10-21
17 Shearwin-Whyatt, L., Dalton, H. E., Foot, N. and Kumar, S. (2006) Regulation of functional diversity within the Nedd4 family by accessory and adaptor proteins. Bioessays. **28**, 617-628
18 Huibregtse, J. M., Scheffner, M., Beaudenon, S. and Howley, P. M. (1995) A family of proteins structurally and functionally related to the E6-AP ubiquitin-protein ligase. Proc. Natl. Acad. Sci. U. S. A. **92**, 2563-2567
19 Kato, Y., Ito, M., Kawai, K., Nagata, K. and Tanokura, M. (2002) Determinants of ligand specificity in groups I and IV WW domains as studied by surface plasmon resonance and model building. J. Biol. Chem. **277**, 10173-10177
20 Sudol, M., Bork, P., Einbond, A., Kastury, K., Druck, T., Negrini, M., Huebner, K. and Lehman, D. (1995) Characterization of the mammalian YAP (Yes-associated protein) gene and its role in defining a novel protein module, the WW domain. J. Biol. Chem. **270**, 14733-14741
21 Kato, Y., Nagata, K., Takahashi, M., Lian, L., Herrero, J. J., Sudol, M. and Tanokura, M. (2004) Common mechanism of ligand recognition by group II/III WW domains: redefining their functional classification. J. Biol. Chem. **279**, 31833-31841
22 Sotgia, F., Lee, H., Bedford, M. T., Petrucci, T., Sudol, M. and Lisanti, M. P. (2001) Tyrosine phosphorylation of beta-dystroglycan at its WW domain binding motif, PPxY, recruits SH2 domain containing proteins. Biochemistry. **40**, 14585-14592
23 Joughin, B. A., Tidor, B. and Yaffe, M. B. (2005) A computational method for the analysis and prediction of protein:phosphopeptide-binding sites. Protein Sci. **14**, 131-139
24 Spindel, O. N., Burke, R. M., Yan, C. and Berk, B. C. (2014) Thioredoxin-interacting protein is a biomechanical regulator of Src activity: key role in endothelial cell stress fiber formation. Circ. Res. **114**, 1125-1132
25 Morales, B., Ramirez-Espain, X., Shaw, A. Z., Martin-Malpartida, P., Yraola, F., Sanchez-Tillo, E., Farrera, C., Celada, A., Royo, M. and Macias, M. J. (2007) NMR structural studies of the ItchWW3 domain reveal that phosphorylation at T30 inhibits the interaction with PPxY-containing ligands. Structure. **15**, 473-483
26 Evans, P. R. and Murshudov, G. N. (2013) How good are my data and what is the resolution? Acta Crystallogr. D Biol. Crystallogr. **69**, 1204-1214
27 McCoy, A. J., Grosse-Kunstleve, R. W., Adams, P. D., Winn, M. D., Storoni, L. C. and Read, R. J. (2007) Phaser crystallographic software. J. Appl. Crystallogr. **40**, 658-674
28 Langer, G., Cohen, S. X., Lamzin, V. S. and Perrakis, A. (2008) Automated macromolecular model building for X-ray crystallography using ARP/wARP version 7. Nat. Protoc. **3**, 1171-1179
29 Emsley, P., Lohkamp, B., Scott, W. G. and Cowtan, K. (2010) Features and development of Coot. Acta Crystallogr. D Biol. Crystallogr. **66**, 486-501

30 Lebedev, A. A., Young, P., Isupov, M. N., Moroz, O. V., Vagin, A. A. and Murshudov, G. N. (2012) JLigand: a graphical tool for the CCP4 template-restraint library. Acta Crystallogr. D Biol. Crystallogr. **68**, 431-440
31 Murshudov, G. N., Skubak, P., Lebedev, A. A., Pannu, N. S., Steiner, R. A., Nicholls, R. A., Winn, M. D., Long, F. and Vagin, A. A. (2011) REFMAC5 for the refinement of macromolecular crystal structures. Acta Crystallogr. D Biol. Crystallogr. **67**, 355-367
32 Adams, P. D., Afonine, P. V., Bunkoczi, G., Chen, V. B., Davis, I. W., Echols, N., Headd, J. J., Hung, L. W., Kapral, G. J., Grosse-Kunstleve, R. W., McCoy, A. J., Moriarty, N. W., Oeffner, R., Read, R. J., Richardson, D. C., Richardson, J. S., Terwilliger, T. C. and Zwart, P. H. (2010) PHENIX: a comprehensive Python-based system for macromolecular structure solution. Acta Crystallogr. D Biol. Crystallogr. **66**, 213-221
33 Chen, V. B., Arendall, W. B., 3rd, Headd, J. J., Keedy, D. A., Immormino, R. M., Kapral, G. J., Murray, L. W., Richardson, J. S. and Richardson, D. C. (2010) MolProbity: all-atom structure validation for macromolecular crystallography. Acta Crystallogr. D Biol. Crystallogr. **66**, 12-21
34 Yang, H., Guranovic, V., Dutta, S., Feng, Z., Berman, H. M. and Westbrook, J. D. (2004) Automated and accurate deposition of structures solved by X-ray diffraction to the Protein Data Bank. Acta Crystallogr. D Biol. Crystallogr. **60**, 1833-1839
35 Gildea, R. J., Bourhis, L. J., Dolomanov, O. V., Grosse-Kunstleve, R. W., Puschmann, H., Adams, P. D. and Howard, J. A. (2011) iotbx.cif: a comprehensive CIF toolbox. J. Appl. Crystallogr. **44**, 1259-1263
36 Winn, M. D. (2003) An overview of the CCP4 project in protein crystallography: an example of a collaborative project. J. Synchrotron. Radiat. **10**, 23-25
37 Klippel, S., Wieczorek, M., Schumann, M., Krause, E., Marg, B., Seidel, T., Meyer, T., Knapp, E. W. and Freund, C. (2011) Multivalent binding of formin-binding protein 21 (FBP21)-tandem-WW domains fosters protein recognition in the pre-spliceosome. J. Biol. Chem. **286**, 38478-38487
38 Qi, S., O'Hayre, M., Gutkind, J. S. and Hurley, J. H. (2014) Structural and biochemical basis for ubiquitin ligase recruitment by arrestin-related domain-containing protein-3 (ARRDC3). J. Biol. Chem. **289**, 4743-4752
39 Shi, H., Asher, C., Chigaev, A., Yung, Y., Reuveny, E., Seger, R. and Garty, H. (2002) Interactions of β and γENaC with Nedd4 can be facilitated by an ERK-mediated phosphorylation. J. Biol. Chem. **277**, 13539-13547
40 Liu, K., Chen, C., Guo, Y., Lam, R., Bian, C., Xu, C., Zhao, D. Y., Jin, J., MacKenzie, F., Pawson, T. and Min, J. (2010) Structural basis for recognition of arginine methylated Piwi proteins by the extended Tudor domain. Proc. Natl. Acad. Sci. U.S.A. 107, 18398-18403
41 Huang, X., Poy, F., Zhang, R., Joachimiak, A., Sudol, M. and Eck, M. J. (2000) Structure of a WW domain containing fragment of dystrophin in complex with beta-dystroglycan. Nat. Struct. Biol. **7**, 634-638
42 Adzhubei, A. A. and Sternberg, M. J. (1993) Left-handed polyproline II helices commonly occur in globular proteins. J. Mol. Biol. **229**, 472-493

43 Dephoure, N., Zhou, C., Villen, J., Beausoleil, S. A., Bakalarski, C. E., Elledge, S. J. and Gygi, S. P. (2008) A quantitative atlas of mitotic phosphorylation. Proc. Natl. Acad. Sci. U. S. A. **105**, 10762-10767
44 Hornbeck, P. V., Kornhauser, J. M., Tkachev, S., Zhang, B., Skrzypek, E., Murray, B., Latham, V. and Sullivan, M. (2012) PhosphoSitePlus: a comprehensive resource for investigating the structure and function of experimentally determined post-translational modifications in man and mouse. Nucleic Acids Res. **40**, D261-270
45 Eck, M. J., Shoelson, S. E. and Harrison, S. C. (1993) Recognition of a high-affinity phosphotyrosyl peptide by the Src homology-2 domain of p56lck. Nature. **362**, 87-91
46 Waksman, G., Shoelson, S. E., Pant, N., Cowburn, D. and Kuriyan, J. (1993) Binding of a high affinity phosphotyrosyl peptide to the Src SH2 domain: crystal structures of the complexed and peptide-free forms. Cell. **72**, 779-790
47 Wu, B., Wang, F., Zhang, J., Zhang, Z., Qin, L., Peng, J., Li, F., Liu, J., Lu, G., Gong, Q., Yao, X., Wu, J. and Shi, Y. (2012) Identification and structural basis for a novel interaction between Vav2 and Arap3. J. Struct. Biol. **180**, 84-95
48 Zhang, Y., Zhang, J., Yuan, C., Hard, R. L., Park, I. H., Li, C., Bell, C. and Pei, D. (2011) Simultaneous binding of two peptidyl ligands by a SRC homology 2 domain. Biochemistry. **50**, 7637-7646
49 Nolte, R. T., Eck, M. J., Schlessinger, J., Shoelson, S. E. and Harrison, S. C. (1996) Crystal structure of the PI 3-kinase p85 amino-terminal SH2 domain and its phosphopeptide complexes. Nat. Struct. Biol. **3**, 364-374
50 Waksman, G., Kominos, D., Robertson, S. C., Pant, N., Baltimore, D., Birge, R. B., Cowburn, D., Hanafusa, H., Mayer, B. J., Overduin, M., Resh, M. D., Rios, C. B., Silverman, L. and Kuriyan, J. (1992) Crystal structure of the phosphotyrosine recognition domain SH2 of v-src complexed with tyrosine-phosphorylated peptides. Nature. **358**, 646-653
51 Xu C, J. J., Bian C, Lam R, Tian R, Weist R, You L, Nie J, Bochkarev A, Tempel W, Tan CS, Wasney GA, Vedadi M, Gish GD, Arrowsmith CH, Pawson T, Yang XJ, Min J. (2012) Sequence-specific recognition of a PxLPxI/L motif by an ankyrin repeat tumbler lock. Sci. Signal. 5, ra39
52 Aragon, E., Goerner, N., Zaromytidou, A. I., Xi, Q., Escobedo, A., Massague, J. and Macias, M. J. (2011) A Smad action turnover switch operated by WW domain readers of a phosphoserine code. Genes & development. 25, 1275-1288
53 Otwinowski, Z., and Minor, W. (1997) Processing of X-ray diffraction data collected in oscillation mode. Method. Enzymol. ***276***, 307-326
54 Perrakis, A., Sixma, T. K., Wilson, K. S. and Lamzin, V. S. (1997) wARP: improvement and extension of crystallographic phases by weighted averaging of multiple-refined dummy atomic models. Acta Crystallogr. D Biol. Crystallogr. **53**, 448-455
55 Kabsch, W. (2010) Xds. Acta Crystallogr. D Biol. Crystallogr. **66**, 125-132
56 Visperas, P. R., Winger, J. A., Horton, T. M., Shah, N. H., Aum, D. J., Tao, A., Barros, T., Yan, Q., Wilson, C. G., Arkin, M. R., Weiss, A. and Kuriyan, J. (2015) Modification by covalent reaction or oxidation of cysteine residues in the tandem-SH2 domains of ZAP-70 and Syk can block phosphopeptide binding. Biochem. J. **465**, 149-161

57 Jaroszewski, L., Rychlewski, L., Li, Z., Li, W. and Godzik, A. (2005) FFAS03: a server for profile--profile sequence alignments. Nucleic Acids Res. **33**, W284-288
58 Canutescu, A. A., Shelenkov, A. A. and Dunbrack, R. L., Jr. (2003) A graph-theory algorithm for rapid protein side-chain prediction. Protein Sci. **12**, 2001-2014
59 Bruno, I. J., Cole, J. C., Kessler, M., Luo, J., Motherwell, W. S., Purkis, L. H., Smith, B. R., Taylor, R., Cooper, R. I. and Harris, S. E. (2004) Retrieval of crystallographically-derived molecular geometry information. J. Chem. Inf. Comp. Sci. **44**, 2133-2144

FIGURE LEGENDS

Figure 1. WW domains of Itch bind to PPxY motifs of TXNIP with different affinities.
(A) Domain structure of human Itch and TXNIP. Itch consists of a C2 domain, four WW domains, and a HECT ubiquitin ligase domain. TXNIP consists of an N-terminal arrestin lobe, a C-terminal arrestin lobe, and a C-terminal tail containing two PPxY motifs. The initial and final residues of each domain are indicated. **(B)** Binding affinities of single or tandem PPxY motifs to individual or tandem WW domains were determined by ITC. All K_d values were calculated from single measurement and errors were estimated by fitting curve. All the ITC assays were performed by VP-ITC microcalorimeter (GE, Inc) except where indicated otherwise.

Figure 2. Structural basis for PPCY motif recognition by tandem WW3-WW4 domain of Itch.
(A) Structure based sequence alignment of WW domains of Itch. Secondary structure elements and residue numbers of WW3 and WW4 are indicated above and below the sequence alignment, respectively. The two conserved tryptophans (W, WW3) or W and tyrosine (Y, WW4) are highlighted in blue. The conserved XP groove and tyrosine groove-forming residues are marked by closed and open black circles, respectively. **(B, C)** Detailed interactions of the PPCY peptide with WW3 (B) and WW4 domain (C) in the (WW3-WW4)-PPCY complex. WW3, WW4 domain and PPCY peptide are shown as cartoon and colored in cyan, pink and yellow, respectively. Interacting residues in WW domains and PPCY peptide are shown in stick mode. Hydrogen bonds are shown as yellow dashes. **(D, E)** Electrostatic potential surface representation of the WW3-PPCY (D) and WW4-PPCY in (WW3-WW4)-PPCY complex (E) (isocontour value of ± 64 kT/e). WW domains are shown in surface representation and PPCY peptides are shown as yellow cartoon or sticks. The conserved XP and tyrosine grooves are shown by black and red circles, respectively.

Figure 3. Phosphorylation of TXNIP blocks its binding to Itch but enables recruitment of SH2 domain containing proteins.
(A) Binding affinities of phosphorylated or un-phosphorylated PPxY motifs to SH2 domains of SHP2 or tandem WW3-WW4 domain of Itch were determined by ITC. All K_d values were calculated from single measurement and errors were estimated by fitting curve. All the ITC assays were performed by VP-ITC microcalorimeter (GE, Inc). **(B)** Overall structure of the C terminal SH2 domains of SHP2 in complex with PPTpY peptide showing the secondary structure notation and binding model of PPTpY peptide. SH2 domains and PPTpY peptide are shown in cartoon mode. **(C)** Schematic representation of the switch model. Phosphorylated PPxY motif disrupts the binding between TXNIP and Itch WW domain (top) but recruits SH2 containing protein SHP2 (bottom). We note that additional data are required to confirm a possible bivalent interaction between tandem PPx(pY) motifs and tandem SH2 domains.

Table 1 Data collection and refinement statistics

complex	Itch (WW3-WW4)-PPCY	SHP2 SH2-PPTpY
PDB code	5CQ2	5DF6
Data reduction		
Radiation wavelength [Å]	0.9792	0.9793
Space group	I222	P21
Cell dimensions a,b,c [Å],α,β,γ [°]	57.28,62.26,67.81,90.00,90.00,90.00	28.47,72.17,62.55,90.00,101.77,90.00
Resolution limits [Å]	45.86-1.40(1.42-1.40)	46.69-1.78(1.82-1.78)
Unique HKLs	24240(1191)	23333(1249)
Completeness [%]	99.9(100.0)	98.5(95.9)
Rsym	0.043(0.927)	0.076(0.526)
I/sigma	25.1(2.0)	11.2(1.4)
Redundancy	7.1(6.5)	3.9(3.3)
Model refinement		
Refinement resolution [Å]	45.86-1.40	46.69-1.78
Reflections used/free	23096/1144	22177/1156
Number of atoms/average B-factor [$Å^2$]	882/25.4	1928/32.0
Protein	616/23.3	1657/31.4
Peptide	193/29.9	154/35.4
Water	55/30.8	110/35.0
Others	18/32.9	7/31.6
R work/free	0.153/0.184	0.194/0.248
RMSD bonds [Å]/angles [°]	0.020/1.8	0.017/1.7
Molprobity Ramachandran favored/outliers [%]	98.92/0.00	98.24/0.00

Figure 1

A

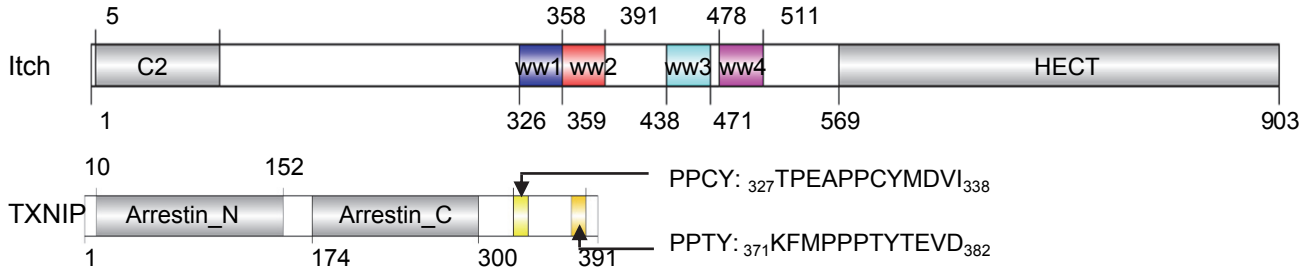

B

	K_d (μM)			
	TXNIP Peptide*			
Itch domain	PPCY	PPTY	2_PPxY_short	2_PPxY_long
WW1	43 ± 4	44 ± 4	--	--
WW2	90 ± 8	65 ± 6	--	--
WW3	431 ± 106	98 ± 7	--	--
WW4	709 ± 148	179 ± 16	--	--
WW1+WW2	--	--	1.0 ± 0.1[a]	--
WW3+WW4	--	--	4.2 ± 0.3/4.9 ± 0.5[a]	10 ± 1

Note: --, not determined; a, determined by Nano ITC (TA, Inc)

*TXNIP Peptide

PPCY: $_{327}$TPEAPPCYMDVI$_{338}$

PPTY: $_{371}$KFMPPPTYTEVD$_{382}$

2_PPxY_short: tandem PPxY peptide with residues 327-338 +371-382

2_PPxY_long: tandem PPxY peptide with residues 327-382

Figure 2

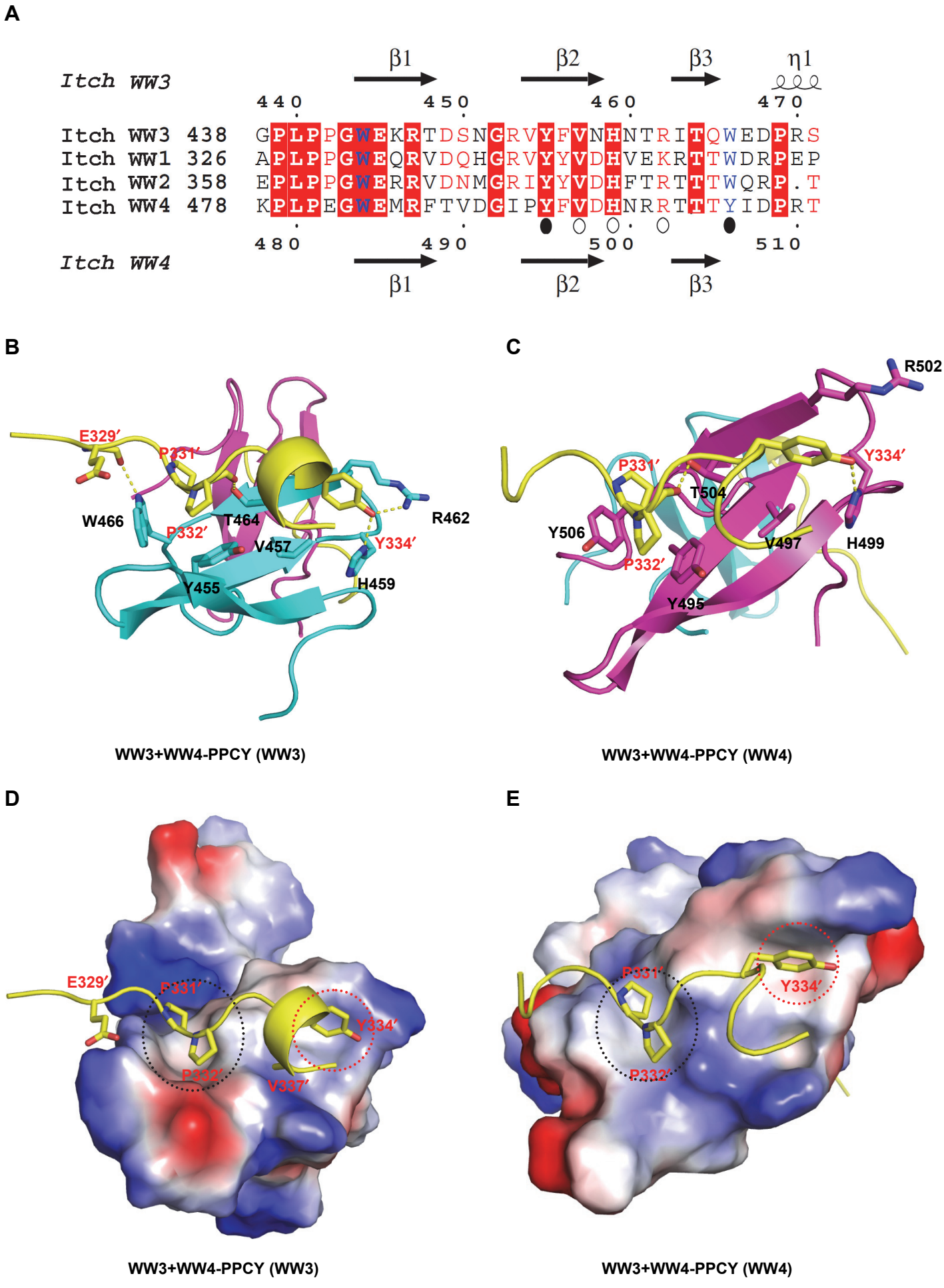
A
Itch WW3
β1
β2
β3
η1
440
450
460
470
Itch WW3 438 GPLPPGWEKRTDSNGRVYFVNHNTRITQWEDPRS
Itch WW1 326 APLPPGWEQRVDQHGRVYYVDHVEKRTTWDRPEP
Itch WW2 358 EPLPPGWERRVDNMGRIYYVDHFTRTTTWQRP.T
Itch WW4 478 KPLPEGWEMRFTVDGIPYFVDHNRRTTTYIDPRT
480
490
500
510
Itch WW4
β1
β2
β3
B
E329′
P331′
W466
T464
P332′
R462
V457
Y334′
Y455
H459
WW3+WW4-PPCY (WW3)
C
R502
P331′
Y334′
T504
Y506
V497
H499
P332′
Y495
WW3+WW4-PPCY (WW4)
D
E329′
P331′
Y334′
P332′
V337′
WW3+WW4-PPCY (WW3)
E
P331′
Y334′
P332′
WW3+WW4-PPCY (WW4)

Figure 3

A

	K_d (μM)			
	TXNIP Peptides*			
	PPCpY	PPTpY	2_PPx(pY)_short	2_PPxY_short
SHP2-N terminal SH2	11 ± 3	5.6 ± 0.3	--	--
SHP2-C terminal SH2	19 ± 3	39 ± 6	--	--
SHP2-tandem SH2	--	--	5.9 ± 0.8	NB
Itch-WW3+WW4	NB	--	--	4.2 ± 0.3

Note: --, not determined; NB, no binding.

*TXNIP Peptide

PPCpY: PPCY peptide with Y324 phosphorylated

PPTpY: PPTY peptide with Y378 phosphorylated

2_PPxY_short: residues 327-338+371-382

2_PPx(pY)_short: residues 327-338+371-382 with Y324 and Y378 phosphorylated